Influence of Molecular Motion on the Accuracy of NMR-Derived Distances. A Molecular Dynamics Study of Two Solvated Model Peptides

Roger Abseher, Susanna Lüdemann, Hellfried Schreiber, and Othmar Steinhauser*

Contribution from the Institut für Theoretische Chemie, Universität Wien, Währinger Strasse 17, A-1090 Wien, Austria

Received August 20, 1993®

Abstract: The law that relates the quotient of two NOE enhancements to the quotient of the corresponding internuclear distances raised to the negative sixth powers is the result of several assumptions concerning molecular motion: elongation and rotation of internuclear distance vectors are assumed to be uncorrelated, and the reorientational motion of all internuclear distance vectors of a given system are described by the same motional model (e.g. rotational diffusion) with the *same* parameters; that is, there is no allowance for individual rotational correlation times for each pair of nuclei. In order to check the validity of these rather restrictive assumptions, we calculated the dipolar correlation functions for a set of internuclear distances in the linear type II β-turn-forming pentapeptide Tyr-Pro-Gly-Asp-Val and the cyclic peptide *N*-triglycin[Lys^8]vasopressin by molecular dynamics simulations (simulation time: more than 2 ns). The structures of these peptides have been determined by combination of ^{1}H–^{1}H-NOE data and molecular dynamics calculations using time-averaged distance constraints. Calculation of the correlation functions has been carried out by simulation in water (long-range interactions have been treated with the method of Ewald summation). We calculated the total dipolar correlation functions as well as the angular part and the distance part of the correlation functions and determined correlation times and generalized order parameters. For the studied set of H–H pairs the assumption of uncorrelated elongation and rotation has turned out to be a suitable approximation, while rotational correlation times are quantities specific for each spin pair of the studied peptides. The relative contribution of reorientation and distance fluctuation to the spectral density is quantitatively analyzed. On the basis of these findings a modified calibration formula is suggested.

Introduction

Nuclear Overhauser effect spectroscopy has become the most valuable tool for determining the three-dimensional solution structure of biological macromolecules. Distance information obtained from nuclear Overhauser effect (NOESY) data is implemented to and combined with various methods for conformational search.[1,2] Different algorithms capable of processing intramolecular distance information have been developed, ranging from distance geometry methods[3-5] and restrained molecular dynamics[6-8] to the Kalman filter method.[9,10]

However, there are several drawbacks that prevent NOESY-derived internuclear distances from being as exact as one would desire. In addition to signal overlap these are basically multispin effects and internal dynamics of the molecule. A considerable amount of work has been spent in estimating the error—as well as in the development of methods for overcoming the limitations—resulting from a neglect of alternative magnetization transfer pathways on the one hand[11-17] and internal dynamics on the other hand.[12,18-27] Molecular dynamics simulations of NMR relaxation parameters[26,28-31]—recently reviewed by G. Wagner[32]—also have addressed these questions.

* Abstract published in *Advance ACS Abstracts*, April 1, 1994.

(1) Torda, A. E.; van Gunsteren, W. F. *Rev. Comput. Chem.* **1992**, *III*, 143–172.
(2) de Vlieg, J.; van Gunsteren, W. F. *Methods Enzymol.* **1991**, *202*, 268–300.
(3) Havel, T. F.; Crippen, G. M.; Kuntz, I. D. *Biopolymers* **1979**, *18*, 73–81.
(4) Braun, W.; Gō, N. *J. Mol. Biol.* **1985**, *186*, 611–626.
(5) Wüthrich, K. *NMR of Proteins and Nucleic Acids*; Wiley-Interscience: New York, 1986; pp 117–199.
(6) Kaptein, R.; Zuiderweg, E. R. P.; Scheek, R. M.; Boelens, R.; van Gunsteren, W. F. *J. Mol. Biol.* **1985**, *182*, 179–182.
(7) Nilsson, L.; Clore, G. M.; Gronenborn, A. M.; Brünger, A. T.; Karplus, M. *J. Mol. Biol.* **1986**, *188*, 455–475.
(8) Clore, G. M.; Brünger, A. T.; Karplus, M.; Gronenborn, A. M. *J. Mol. Biol.* **1986**, *191*, 523–551.
(9) Altman, R. B.; Jardetzky, O. *Methods Enzymol.* **1989**, *177*, 218–246.
(10) Pachter, R.; Altman, R. B.; Jardetzky, O. *J. Magn. Reson.* **1990**, *89*, 578–584.
(11) Olejniczak, E. T.; Gampe, R. T., Jr.; Fesik, S. W. *J. Magn. Reson.* **1986**, *67*, 28–41.
(12) Lane, A. N. *J. Magn. Reson.* **1988**, *78*, 425–439.
(13) Koehl, P.; Lefèvre, J.-F. *J. Magn. Reson.* **1990**, *86*, 565–583.
(14) Borgias, B. A.; Gochin, M.; Kerwood, D. J.; James, T. L. *Prog. Nucl. Magn. Reson. Spectrosc.* **1990**, *22*, 83–100.
(15) Post, C. B.; Meadows, R. P.; Gorenstein, D. G. *J. Am. Chem. Soc.* **1990**, *112*, 6796–6803.
(16) Thomas, P. D.; Basus, V. J.; James, T. L. *Proc. Natl. Acad. Sci. U.S.A.* **1991**, *88*, 1237–1241.
(17) Clore, G. M.; Robien, M. A.; Gronenborn, A. M. *J. Mol. Biol.* **1993**, *231*, 82–102.
(18) Braun, W.; Bösch, C.; Brown, L. R.; Gō, N.; Wüthrich, K. *Biochim. Biophys. Acta* **1981**, *667*, 377–396.
(19) Olejniczak, E. T.; Dobson, C. M.; Karplus, M.; Levy, R. M. *J. Am. Chem. Soc.* **1984**, *106*, 1923–1930.
(20) Lefèvre, J.-F.; Lane, A. N.; Jardetzky, O. *Biochemistry* **1987**, *26*, 5076–5090.
(21) Baleja, J. D.; Moult, J.; Sykes, B. D. *J. Magn. Reson.* **1990**, *87*, 375–384.
(22) Koning, T. M. G.; Boelens, R.; Kaptein, R. *J. Magn. Reson.* **1990**, *90*, 111–123.
(23) Duben, A. J.; Hutton, W. C. *J. Am. Chem. Soc.* **1990**, *112*, 5917–5924.
(24) Koning, T. M. G.; Boelens, R.; van der Marel, G. A.; van Boom, J. H.; Kaptein, R. *Biochemistry* **1991**, *30*, 3787–3797.
(25) Fejzo, J.; Krezel, A. M.; Westler, W. M.; Macura, S.; Markley, J. L. *Biochemistry* **1991**, *30* (16), 3807–3811.
(26) Brüschweiler, R.; Roux, B.; Blackledge, M.; Griesinger, C.; Karplus, M.; Ernst, R. R. *J. Am. Chem. Soc.* **1992**, *114*, 2289–2302.
(27) Post, C. B. *J. Mol. Biol.* **1992**, *224*, 1087–1101.
(28) Palmer, A. G., III; Case, D. A. *J. Am. Chem. Soc.* **1992**, *114*, 9059–9067.
(29) Kördel, J.; Teleman, O. *J. Am. Chem. Soc.* **1992**, *114*, 4934–4946.
(30) Chandrasekhar, I.; Clore, G. M.; Szabo, A.; Gronenborn, A. M.; Brooks, B. R. *J. Mol. Biol.* **1992**, *226*, 239–250.
(31) Daragan, V. A.; Mayo, K. H. *Biochemistry* **1993**, *32*, 11488–11499.
(32) Wagner, G. *Curr. Opin. Struct. Biol.* **1993**, *3*, 748–754.

0002-7863/94/1516-4006$04.50/0

In the present work we address the effects of molecular motion on the determination of intramolecular distances. The relaxation processes giving rise to the nuclear Overhauser effect (NOE) are triggered by the molecular motion of the system under consideration. The central quantity representing the link between molecular motion and dipolar relaxation rate constants is the autocorrelation function of the internuclear distance vector (in the following referred to as the dipolar correlation function). In order to facilitate the treatment of the dipolar correlation function, physical models describing molecular motion are adopted. It is common practice to extract internuclear distances from NOE data by using two basic assumptions for molecular motion: (1) Elongation and rotation of the internuclear distance vector are assumed to be uncorrelated, and (2) the reorientational correlation functions of all internuclear distance vectors are described by a uniform, usually exponential, time behavior. These assumptions result in a simple relation between the cross relaxation rate constant and the internuclear distance, thus permitting the quantification of intramolecular distances.

The goal of our work is to check the validity of these assumptions. For this purpose two peptide systems have been chosen: the cyclic dodecapeptide Gly$^{\gamma}$-Gly$^{\beta}$-Gly$^{\alpha}$-Cys^{1}-Tyr^{2}-Phe^{3}-Gln^{4}-Asn^{5}-Cys^{6}-Pro^{7}-Lys^{8}-Gly^{9}-NH$_2$ cyclic (1 → 6) disulfide, which is the *N*-triglycin derivative of [Lys^{8}]vasopressin (tgvp), and the linear, predominantly type II β-turn-forming pentapeptide Tyr-Pro-Gly-Asp-Val (YPGDV). YPGDV is one of the peptide fragments which have been systematically examined with regard to β-turn folding and stability by H. J. Dyson et al.[33] The ^{1}H-NMR data for tgvp are from H. Sterk's laboratory.[34]

We determined the structures of these peptides using restrained molecular dynamics with *time-averaged* distance constraints (MD-tar), a concept introduced by A. Torda et al.[35,36]

As structure and dynamics of flexible molecules are very sensitive to the environment of the simulation,[37-39] we recorded the dipolar correlation functions under the following conditions: (1) A large number of solvent molecules are explicitly present in the simulation. (2) In order to ensure a realistic description of the dielectric environment, long-range Coulomb interactions have been treated with the method of Ewald summation. For both systems we performed simulations of more than 2 ns duration for the acquisition of the correlation functions of a set of interproton distance vectors.

Theory

The nuclear Overhauser effect (NOE) is a kinetic phenomenon involving magnetization transfer between nuclei. The following equation governs the relaxation of a two-spin system under idealized conditions (spin–lattice relaxation is assumed to be the only relaxation mechanism):[40]

$$\frac{dM_z^I}{dt} = -(M_z^I - M_{z,0}^I)(2W_{1I} + W_{2IS} + W_{0IS}) - (M_z^S - M_{z,0}^S)(W_{2IS} - W_{0IS}) \quad (1)$$

M_z^I and M_z^S are the z-magnetizations of spin I and spin S, respectively, $M_{z,0}^I$ and $M_{z,0}^S$ are the corresponding equilibrium values, and W_{1I}, W_{2IS}, and W_{0IS} are the probabilities for a single quantum transition of spin I, for a double quantum transition and for a zero quantum transition, respectively. The expression $(2W_{1I} + W_{2IS} + W_{0IS})$ is also called the dipolar longitudinal relaxation rate constant ρ_{IS}, and $(W_{2IS} - W_{0IS})$ is the cross relaxation rate constant σ_{IS}. The initial buildup of NOEs in a kinetic experiment involves σ_{IS} as the rate constant:

$$f_I\{S\}(t) = (\gamma_S/\gamma_I)\sigma_{IS}t \quad (2)$$

$f_I\{S\}$ is the NOE enhancement, i.e. the fractional change in the intensity of I on saturating S; $f_I\{S\} = (M_z^I - M_{z,0}^I)/M_{z,0}^I$.

Expressions for the transition probabilities in eq 1 are derived from quantum mechanical time-dependent perturbation theory.[40,41]

$$\overline{W_{mn}} = (1/\hbar^2)\int \overline{V_{mn}^*(0)V_{mn}(t)}\, dt \quad (3)$$

The letters m and n stand for the initial and the final state of the spin system, and V_{mn} are the matrix elements of the dipolar Hamiltonian

$$\hat{V} = (\mu_0/4\pi)\hbar\gamma_I\gamma_S(1/r_{IS}^3)[\hat{I}\hat{S} - (3/r_{IS}^2)(\hat{I}\vec{r}_{IS})(\hat{S}\vec{r}_{IS})] \quad (4)$$

where $\vec{r}_{IS}$ is the internuclear distance vector in the laboratory coordinate system and r_{IS} is the length of $\vec{r}_{IS}$. Combining eqs 3 and 4, one gets

$$\overline{W_{mn}} = k_{mn}\int C_{IS}^{DD}(t)e^{-i\omega_{mn}t}\, dt \quad (5)$$

where k_{mn} is a constant depending on the respective transition and $C_{IS}^{DD}(t)$ is the dipolar correlation function.

$$C_{IS}^{DD}(t) = \overline{r_{IS}^{-3}(0)r_{IS}^{-3}(t)\cdot P_2(\vec{\mu}(0)\cdot\vec{\mu}(t))} \quad (6)$$

P_2 is the second Legendre polynomial and $\vec{\mu}$ the unit vector pointing along $\vec{r}_{IS}$.

Without assumptions there is no direct route to an average internuclear distance. Therefore, the traditional approach simplifies the dipolar correlation function $C^{DD}(t)$ in the following way: First, elongation and rotation are assumed to be uncoupled; that is, they are considered to be independent processes. There is no requirement for rotation and elongation to occur on different time scales for this separation. There will be such a requirement, however, in the later stage of the derivation of the simple calibration formula eq 13, namely, for the step from eq 9 to eq 10. Uncoupled rotation and elongation permit a factoring of the dipolar correlation function in an angular and a distance part:

$$C^{DD}(t) = C_{rot}^{DD}(t)\, C_{dis}^{DD}(t) \quad (7)$$

For $C_{rot}^{DD}(t)$ various models may be introduced, provided that they use parameters that are the same for all distance vectors within a molecule. This is a requirement for the calibration method used in analyzing NOESY spectra (a well-characterized NOE with known distance between the nuclei is used as an internal intensity standard; cf. eq 13). Of course such a uniform time behavior is a severe restriction of the reorientational motion model, and our results clearly rule out such a model as a candidate for a proper description of molecular motion. For easy tractability usually isotropic rotational diffusion is chosen. Thus, one obtains[42]

$$C^{DD}(t) = e^{-t/\tau_{rot}}C_{dis}^{DD}(t) \quad (8)$$

There are two possible arguments for this assumption: (1) Overall tumbling is the only contribution to rotational motion; reorien-

(33) Dyson, H. J.; Rance, M.; Houghten, R. A.; Lerner, R. A.; Wright, P. E. *J. Mol. Biol.* **1988**, *201*, 161–200.
(34) Zieger, G.; Andreae, F.; Sterk, H. *Magn. Reson. Chem.* **1991**, *29*, 580–586.
(35) Torda, A. E.; Scheek, R. M.; van Gunsteren, W. F. *Chem. Phys. Lett.* **1989**, *157* (4), 289–294.
(36) Torda, A. E.; Scheek, R. M.; van Gunsteren, W. F. *J. Mol. Biol.* **1990**, *214*, 223–235.
(37) Schreiber, H.; Steinhauser, O. *Biochemistry* **1992**, *31* (25), 5856–5860.
(38) Schreiber, H.; Steinhauser, O. *Chem. Phys.* **1992**, *168*, 75–89.
(39) Schreiber, H.; Steinhauser, O. *J. Mol. Biol.* **1992**, *228*, 909–923.
(40) Neuhaus, D.; Williamson, M. *The Nuclear Overhauser Effect*; Verlag Chemie: Weinheim, 1989.
(41) Atkins, P. W. *Molecular Quantum Mechanics*, 2nd ed.; Oxford University Press: Oxford, 1983; Chapter 7.
(42) Tropp, J. *J. Chem. Phys.* **1980**, *72* (11), 6035–6043.

tational motion in a molecule-fixed ("internal") coordinate frame is negligible. τ_{rot} would then be equal to $1/6R$, where R is the rotational diffusion constant for the overall tumbling motion of the molecule. (2) Internal motion *does* contribute, but there are no individual correlation times for different distance vectors within a molecule. (This is not a very likely situation.) In this case τ_{rot} is given by $\tau_{rot}^{-1} = \tau_{rot,ov}^{-1} + \tau_{rot,int}^{-1}$, where $\tau_{rot,ov} = 1/6R$ and $\tau_{rot,int}$ is the effective rotational correlation time in the internal coordinate frame. Furthermore, it is assumed that distance correlation reaches its plateau value in a short time interval as compared to reorientational motion; a specific model of such a behavior may be[40,43]

$$C_{dis}^{DD}(t) = (\overline{r_{IS}^{-3}})^2 + [\overline{r_{IS}^{-6}} - (\overline{r_{IS}^{-3}})^2]e^{-t/\tau_{dis}} \quad (9)$$

At this point there are two quantities *specific* for each internuclear vector: r_{IS} and τ_{dis}. In order to get rid of τ_{dis} (a requirement for proceeding), τ_{dis} is assumed to be small as compared to τ_{rot}. Doing the Fourier transformation in eq 5, we obtain for the cross relaxation rate constant

$$\sigma_{IS} = (1/10)(\mu_0/4\pi)^2\hbar^2\gamma_I^2\gamma_S^2(\overline{r_{IS}^{-3}})^2 f(\tau_{rot}) \quad (10)$$

r_{IS} is now—by assumption—the only quantity which reflects the individual behavior of a specific internuclear distance vector $\vec{r}_{IS}$, as a uniform rotational time behavior was assumed. $f(\tau_{rot})$ is given by

$$f(\tau_{rot}) = \frac{6\tau_{rot}}{1 + (\omega_I + \omega_S)^2\tau_{rot}^2} - \frac{\tau_{rot}}{1 + (\omega_I - \omega_S)^2\tau_{rot}^2} \quad (11)$$

Relying on eq 10, calibration becomes feasible:

$$\sigma_{ij}/\sigma_{kl} = (\overline{r_{ij}^{-3}})^2/(\overline{r_{kl}^{-3}})^2 \quad (12)$$

where (i,j) and (k,l) are two different spin pairs, one of them with a well-known distance r between the nuclei. As the distribution functions of the internuclear distances are usually unknown, the averaging cannot be performed explicitly. Thus, eq 12 is rewritten in terms of effective distances:

$$\sigma_{ij}/\sigma_{kl} = r_{ij,eff}^{-6}/r_{kl,eff}^{-6} \quad (13)$$

This simple formula is the result of rather restrictive assumptions concerning molecular motion, which are briefly summarized in the following: (i) the product approximation represented by eq 7, (ii) the postulation of a uniform time behavior of the rotational motion, e.g. eq 8, and (iii) elongation and rotation are assumed to take place on different time scales (requirement for eq 10). For comparison, Lipari and Szabo[44,45] also factor the dipolar correlation function, namely, in a part arising from overall motion (C_{ov}^{DD}) and a part arising from internal motions (C_{int}^{DD}). This is physically reasonable, but entirely different from eq 7, because there is no one-to-one correspondence between overall and internal motion on the one hand and rotation and elongation on the other hand. Internal motions usually *do* contribute to the distance part as well as to the angular part of the dipolar correlation function. Thus, C_{int}^{DD} *a priori* cannot be equated to C_{dis}^{DD}. Furthermore, the formalisms for the interpretation of NMR relaxation data introduced by Jardetzky et al.[46-48] or Lipari and Szabo[44,45] respectively describe the motion of each distance vector in the internal coordinate frame by an individual rotational correlation time, as opposed to eq 13.

In order to find out how good the total dipolar correlation function can be approximated using a uniform rotational correlation time and separately averaged distance and angular parts, we recorded $C^{DD}(t)$ as well as $C_{dis}^{DD}(t)$ and $C_{rot}^{DD}(t)$ during the MD simulations of YPGDV and *N*-triglycin[Lys[8]]vasopressin.

Programs and Methods

For generating the initial *all-trans* configurations of the peptides, we used the INSIGHTII molecular modeling package (Biosym). The molecular topologies have been constructed with the program PROGMT of the GROMOS86 package[49] using the 37D4 version of the force field (vacuum simulations) or the 37C4 version (solvated simulations), respectively. For setting up the systems for the solvated simulations, we used the GROMOS programs PROBOX and PROION. The final rectangular boxes were 3.0 × 3.0 × 3.5 nm (tgvp) and 2.8 × 2.8 × 2.8 nm (YPGDV) in size and contained 983 and 712 SPC-type water molecules, respectively.

All MD simulations were carried out with a modified version of the program PROMD, originally part of the GROMOS86 package. The subroutines for computing the neighbor lists and calculating nonbonded interactions were replaced by a self-written code.

In order to eliminate high-order vibrational motions, the SHAKE algorithm[50] was applied with a time step of 2 fs. The temperature was kept near 300 K by an appropriate scaling of the atomic velocities.[51] For economic reasons, the neighbor-list technique was exploited using an updating frequency of 10 time steps.

Self-written subroutines for calculating time-averaged distance restraint forces and the dipolar correlation functions have been added to our version of PROMD.

A. Restrained Molecular Dynamics. The NOE distance information has been taken into account using the following type of restraint potential:

$$U_{restr} = \lambda_1(\bar{r} - r_{min})^2 \; \forall \; \bar{r} < r_{min} \quad (14)$$

$$U_{restr} = 0 \; \forall \; r_{min} \le \bar{r} \le r_{max} \quad (15)$$

$$U_{restr} = \lambda_2(\bar{r} - r_{max})^2 \; \forall \; \bar{r} > r_{max} \quad (16)$$

where r_{max} is the upper bound, r_{min} the lower bound of the respective NOE, and λ_1 and λ_2 are the force constants. This is the commonly used harmonic restraint potential with one exception: Instead of involving the instantaneous internuclear distance $r(t)$, this potential restrains the average distance $\bar{r}(t)$, given by the following formula:[35,36]

$$\bar{r}(t) = [(1/\tau)\int_0^t \exp(-t'/\tau)r(t-t')^{-3}\,dt']^{-1/3} \quad (17)$$

In other words, a memory function $e^{-t'/\tau}$ is employed with τ as a characteristic decay time, which has been set to 1.25 ps. Without the memory function the average value of the internuclear distance ($\bar{r}$) would become increasingly insensitive to the instantaneous values of the internuclear distance (r). Using an exponential memory function one can calculate $\bar{r}(t)$ from $\bar{r}(t - \Delta t)$ recursively:[35]

$$\bar{r}(t)^{-3} = \bar{r}(t - \Delta t)^{-3}e^{-\Delta t/\tau} + r(t)^{-3}(1 - e^{-\Delta t/\tau}) \quad (18)$$

where Δt is the time step of the simulation.

As the 37C4 and 37D4 versions of the GROMOS force field consider explicitly only those hydrogens that are attached to polar groups, the coordinates of hydrogens attached to aliphatic and aromatic carbon atoms have to be generated separately. The restraint force acting on such a hydrogen atom is then redistributed for each time step to the neighboring atoms explicitly present in the force field.[49] In the following we sometimes refer to the *restraint-driven* structure generation process as "folding".

(43) Kessler, H.; Griesinger, C.; Lautz, J.; Müller, A.; van Gunsteren, W. F.; Berendsen, H. J. C. *J. Am. Chem. Soc.* **1988**, *110*, 3393–3396.
(44) Lipari, G.; Szabo, A. *J. Am. Chem. Soc.* **1982**, *104*, 4546–4559.
(45) Lipari, G.; Szabo, A. *J. Am. Chem. Soc.* **1982**, *104*, 4559–4570.
(46) King, R.; Jardetzky, O. *Chem. Phys. Lett.* **1978**, *55* (1), 15–18.
(47) Jardetzky, O.; Ribiero, A. A.; King, R. *Biochem. Biophys. Res. Commun.* **1980**, *3*, 883.
(48) Ribiero, A. A.; King, R.; Restivo, Ch.; Jardetzky, O. *J. Am. Chem. Soc.* **1980**, *102*, 4040–4051.
(49) van Gunsteren, W. F.; Berendsen, H. J. C. *GROningen MOlecular Simulation (GROMOS) library manual*; Biomos: Groningen, The Netherlands, 1987.
(50) van Gunsteren, W. F.; Berendsen, H. J. C. *Mol. Phys.* **1977**, *34*, 1311–1327.
(51) Berendsen, H. J. C.; Postma, J. P. M.; DiNola, A.; Haak, J. R. *J. Chem. Phys.* **1984**, *81*, 3684–3690.

This is not to be confused with the *autonomous* folding process of a nascent peptide chain in a natural environment or a simulation of such a process.

We divided the available structural information about the peptides into two groups. One data set—consisting exclusively of NOE distances determining the peptides' main chain conformation—has been used as input for time-averaged constraints. The other *independent* data set—^3J coupling constants, dihedral angles, nontrivial hydrogen bonds—has been used as a reference for checking the modeled structures.

"Folding" of the peptides has been performed *in vacuo*. It required 200 ps at maximum. The force constant λ_2 (eq 16) was set equal to 1000 or 2000 (in some cases 5000) kJ mol^{-1} nm^{-2}. Comparison with the force constant of the covalent $^{\alpha}$C–N bond, which is 188 407 kJ mol^{-1} nm^{-2} in the GROMOS 37D4 force field, reveals that the force constants for time-averaged distance restraining are evidently low. The force constant λ_1 (eq 14) was set to 0 in order to avoid further restriction of the systems' dynamics. In addition van der Waals repulsion as such prevents atoms from coming too close to each other.

In the case of *N*-triglycin[Lys^8]vasopressin a dihedral restraint potential for fixing the trans configuration of the peptide bond between Cys^6 and Pro^7 turned out to be necessary. The force constant of the native dihedral potential was enlarged from 33.5 to 63.5 kJ mol^{-1} during the intermediate "folding" period. We started with the reduced form of the peptide; that is, there was no disulfide bond. First, we modeled the part of the molecule constituting the ring. When all distance constraints inside the ring had been fulfilled, we closed the disulfide bond: The two sulfhydryl groups were brought near to each other by introducing a further (fictitious and not experimental) distance constraint. By this method we made sure that the topological constraint imposed by the disulfide bond is not present in the early stage of restraining. After the closure of the ring we began to apply constraints concerning the residues outside the ring.

After "folding" we performed at least 200 ps simulation runs under the same conditions (*in vacuo*, distance constraint forces still active; the Cys-Pro dihedral potential force constant has been reset to its "native" value). During this period we acquired time-averaged structural parameters needed for comparison with the reference data set. (We preferred this method to an analysis of a few snapshots.)

Finally, we changed the environment and performed solvated simulations using only the native force field (no constraints present). During simulation periods of more than 2 ns we observed the kinetic stability of the folded structures and recorded the dipolar correlation functions of a set of internuclear distance vectors.

B. Dipolar Correlation Function. The normalized dipolar correlation function is given by

$$C^{DD}(t) = \overline{r_{IS}^{-3}(0) r_{IS}^{-3}(t) \cdot P_2(\vec{\mu}(0)\cdot\vec{\mu}(t))} / \overline{r_{IS}^{-6}} \qquad (19)$$

In addition we recorded the (normalized) rotational part,

$$C_{rot}^{DD}(t) = \overline{P_2(\vec{\mu}(0)\cdot\vec{\mu}(t))} \qquad (20)$$

and the normalized distance part,

$$C_{dis}^{DD}(t) = \overline{r_{IS}^{-3}(0) r_{IS}^{-3}(t)} / \overline{r_{IS}^{-6}} \qquad (21)$$

of the total dipolar correlation function separately. r_{IS} and $\vec{\mu} = \vec{r}_{IS}/|\vec{r}_{IS}|$ have been calculated in intervals of 0.02 ps. The sliding time window within which the autocorrelation functions are calculated was chosen to be T = 30 ps.

The calculations have been performed on local workstations (HP 9000/720, IBM RS6000/550) as well as on an IBM ES9021 and on an IBM RS6000/550 cluster, both located at the Computer Center of the University of Vienna.

Product Approximation Error. In order to estimate the error arising from factoring the total dipolar correlation function into an angular and a distance part (eq 7), the product of $C_{dis}^{DD}(t)$ and $C_{rot}^{DD}(t)$ has been calculated and compared to the total dipolar correlation function. We defined the error due to the product approximation in the following way:

$$\langle \text{error(PA)} \rangle = \frac{1}{T}\int_0^T \frac{C_{dis}^{DD}(t)\, C_{rot}^{DD}(t) - C^{DD}(t)}{C^{DD}(t)}\, dt \qquad (22)$$

where again T is the size of time window of the correlation function (30 ps). We use an integral error because NMR integrates over the fast time scales. A time scale is considered to be fast if its correlation time is much smaller than $(1/\omega)$, where ω is the frequency of the transitions by which dipolar cross relaxation occurs.

Motional Parameters. We extracted motional parameters from the correlation functions by fitting them to target function $g(t)$. As the simulated correlation functions clearly show multiexponential time behavior, we used target functions which allow for more than one underlying motional process. Assuming these processes to occur independently from each other, the composed correlation function $g(t)$ may be written as a product of simple correlation functions in the following way:

$$g(t) = \prod_i [S_i^2 + (1 - S_i^2)e^{-t/\tau_i}] \qquad (23)$$

The expression in square brackets is the general form of the time correlation function of a diffusive motional process, e.g. rotational diffusion or diffusive-like jump processes, with the correlation time τ_i and the generalized order parameter S_i^2, which lies within the interval [0,1]. These parameters *a priori* need not be physically meaningful. For our fits i runs from 1 to 2 or from 1 to 3. In the case of the total dipolar correlation function and its angular part, one of the generalized order parameters is equal to 0, because the overall tumbling motion is not spatially restricted. Irrespective of the overall tumbling's physical characteristic, we account for it with a single parameter τ_{snr} (spatially not restricted component of molecular motion), which potentially is specific for a given NOE. The target functions in the following equations (24–26) have been used for the fits of the total correlation function and its angular part. If i runs up to 2, we obtain correlation functions of an analytical form as proposed by Lipari and Szabo.[44]

$$g(t) = [S^2 + (1 - S^2)e^{-t/\tau_{int}}]e^{-t/\tau_{snr}} \qquad (24)$$

If i runs up to 3, the target function becomes

$$g(t) = [S_1^2 + (1 - S_1^2)e^{-t/\tau_{int,1}}][S_2^2 + (1 - S_2^2)e^{-t/\tau_{int,2}}]e^{-t/\tau_{snr}} \qquad (25)$$

This is equivalent to

$$g(t) = S_1^2S_2^2e^{-t/\tau_{snr}} + S_2^2(1 - S_1^2)e^{-t(\tau_{int,1}^{-1}+\tau_{snr}^{-1})} + (1 - S_2^2)(1 - S_1^2)e^{-t(\tau_{int,1}^{-1}+\tau_{int,2}^{-1}+\tau_{snr}^{-1})} + (S_1^2 - S_1^2S_2^2)e^{-t(\tau_{int,2}^{-1}+\tau_{snr}^{-1})} \qquad (26)$$

If $\tau_{int,1} \ll \tau_{int,2} \ll \tau_{snr}$, eq 26 approximates to

$$g(t) = S^2e^{-t/\tau_{snr}} + (1 - S_1^2)e^{-t/\tau_{int,1}} + (S_1^2 - S^2)e^{-t/\tau_{int,2}} \qquad (27)$$

where $S^2 = S_1^2S_2^2$. This type of correlation function has been proposed by Clore et al.[52,53] for those cases where the Lipari–Szabo approach fails to account for the NMR relaxation data. Again we emphasize that we permit τ_{snr} to be NOE-specific. For the fits of the distance correlation functions, target functions like eq 23 have been used. None of the two respectively three-order parameters have been set to 0, as distance correlation functions in principle do not vanish asymptotically.

We used two criteria for the assessment of the goodness-of-fit. As a first step, we inspected the sum of least squares,

$$\sum_{t_i=0}^{T} (g(t_i) - C(t_i))^2 \qquad (28)$$

which is precisely the quantity minimized by the fitting algorithm. $C(t)$ is the (normalized) correlation function under consideration, i.e. one of the following three: $C^{DD}(t)$, $C_{dis}^{DD}(t)$, or $C_{rot}^{DD}(t)$. t_i runs from 0 to T = 30 ps in 0.02-ps steps. The sums of least squares for each fit are shown in Tables 7 and 8. In order to be compatible with the classical theory of

(52) Clore, G. M.; Driscoll, P. C.; Wingfield, P. T.; Gronenborn, A. M. *Biochemistry* **1990**, *29*, 7387–7401.

(53) Clore, G. M.; Szabo, A.; Bax, A.; Kay, L. E.; Driscoll, P. C.; Gronenborn, A. M. *J. Am. Chem. Soc.* **1990**, *112*, 4989–4991.

Table 1. Results of Folding tgvp *in vacuo* (Column 5) and of the Subsequent Solvated Simulation (Column 6)[a]

NOE[b]	class[b]	intensity[c]	λ_2[d]	$\bar{r}$/nm (200-ps MD-tar[e])	$\bar{r}$/nm (2.4-ns MD)	remark
$d_{\alpha\alpha}^{CC}(1,6)$	long-range	s	1000	0.218 ± 0.014	0.238 ± 0.027	in the ring
$d_{\alpha N}^{CY}(1,2)$	sequential	m	1000	0.202 ± 0.007	0.206 ± 0.013	in the ring
$d_{\alpha N}^{YF}(2,3)$	sequential	m	1000	0.207 ± 0.021	0.209 ± 0.015	in the ring
$d_{\alpha N}^{FQ}(3,4)$	sequential	s	2000	0.200 ± 0.009	0.199 ± 0.013	in the ring
$d_{\alpha N}^{QN}(4,5)$	sequential	s	2000	0.319 ± 0.010	0.339 ± 0.011	in the ring
$d_{\alpha N}^{NC}(5,6)$	sequential	s	1000	0.209 ± 0.009	0.202 ± 0.013	in the ring
$d_{\alpha\delta}^{CP}(6,7)$	sequential	s	1000	0.408 ± 0.004	0.410 ± 0.013	trans specific
$d_{\alpha N}^{PK}(7,8)$	sequential	s	1000	0.205 ± 0.007	0.205 ± 0.015	outside the ring

[a] NOE constraints used and corresponding mean internuclear distances. λ_2: this column shows the *final* values of the force constant (see text). λ_1 is always 0. *All* force constants of restraint potentials are 0 during the 2.4-ns solvated simulation. $\bar{r}$ is the average internuclear distance (sampling interval in both cases 0.02 ps). $d_{\alpha\delta}^{CP}(6,7)$ is specific for the trans configuration of the Cys–Pro peptide bond and the only distance that markedly violates the distance constraint. [b] Notation and classification follows ref 56. [c] Possible entries: s (strong), m (medium), w (weak). [d] In kJ mol^{-1} nm^{-2}. [e] Molecular dynamics with time-averaged restraints (tar).

Table 2. Results of Folding YPGDV *in vacuo* (Column 5) and of the Subsequent Solvated Simulation (Column 6).[a]

NOE	class	intensity	λ_2[b]	$\bar{r}$/nm (200-ps MD-tar)	$\bar{r}$/nm (2.18-ns MD)
$d_{\alpha N}^{PG}(2,3)$	sequential	s	1000	0.202 ± 0.008	0.205 ± 0.015
$d_{NN}^{GD}(3,4)$	sequential	s	5000	0.265 ± 0.016	0.361 ± 0.052
$d_{\alpha\delta}^{YP}(1,2)$	sequential	m	1000	0.304 ± 0.011	0.271 ± 0.021
$d_{\alpha N}^{GD}(3,4)$	sequential	m	1000	0.306 ± 0.004	0.270 ± 0.019
$d_{\alpha N}^{PD}(2,4)$	medium-range	w	5000	0.393 ± 0.010	0.503 ± 0.060
$d_{NN}^{DV}(4,5)$	sequential	w	1000	0.421 ± 0.015	0.427 ± 0.024

[a] NOE constraints used and corresponding mean internuclear distances. $\bar{r}$ is the average internuclear distance (sampling interval 0.02 ps). [b] In kJ mol^{-1} nm^{-2}.

probability, we also calculated the chi-squared probability function Q:[54]

$$Q(\nu/2,\chi^2/2) = \frac{1}{\int_0^\infty e^{-t}t^{(\nu/2-1)}\,dt}\int_{\chi^2/2}^\infty e^{-t}t^{(\nu/2-1)}\,dt \qquad (29)$$

where χ^2 is given by

$$\chi^2 = \sum_{t_i=0}^{T}\frac{(g(t_i)-\mathbf{C}(t_i))^2}{\sigma^2(t_i)} \qquad (30)$$

with the variance

$$\sigma^2(t_i) = (2\tau/L)[1-\mathbf{C}(t_i)]^2 \qquad (31)$$

given by Zwanzig and Ailawadi.[55] τ is the mean relaxation time and L the trajectory length. ν in eq 29 is the number of degrees of freedom, i.e. the number of data points reduced by the number of parameters of the correlation function. The chi-squared probability function yields the probability that even for a "correct" model the chi-squared value will exceed that of the given fit. Q is a value between 0.0 and 1.0. Even for the worst cases, i.e. large values for $\sum_{t_i}(g(t_i)-\mathbf{C}(t_i))^2$ or small values of σ^2, respectively, Q equals 1.0 within machine precision. This demonstrates the high quality of the fits. Therefore, for practical purposes, it makes no difference if one uses the simulated correlation functions or their fitted counterparts.

Results

A. Structure Determination. The NOE distances used as constraints have been taken from refs 34 and 33. The NOE subsets chosen for modeling are shown in Tables 1 and 2. We applied distance constraints to main chain hydrogen atoms only. Exceptionally, we included a single NOE specific for the trans configuration of the X–Pro peptide bond ($d_{\alpha\delta}^{XP}$), which is present in both systems. As one can assume that the side chains of small systems like the two peptides studied here do not exhibit well-defined conformations, no attempt has been made to restrict their dynamics. The force constant λ_2 of the restraint potential (eq 16) was set to 1000 kJ mol^{-1} nm^{-2} for each NOE. In a few cases λ_2 had to be raised to 2000 kJ mol^{-1} nm^{-2} (tgvp) or 5000 kJ mol^{-1} nm^{-2} (YPGDV). Tables 1 and 2 show the final values of λ_2.

After "folding", the structures were subjected to a further 200-ps simulation *in vacuo* with constraint potentials unchanged. During this time we acquired averaged structural parameters, i.e. NOE distances, main chain dihedral angles, and hydrogen bonds. Apart from NOE distances these data have not been used as an input for structure determination. The data in Tables 3 and 4 show that the 200-ps time average of the folded structures is compatible with the experimental data. Figures 1 and 2 (continuous lines) show distribution functions of main chain dihedral angles for several residues in tgvp and YPGDV. In addition, the characteristic hydrogen bonds (tgvp, ^{3}PheCO–^{5}AsnNH; YPGDV, ^{1}TyrCO–^{4}AsnNH) formed spontaneously at the end of the folding procedure (Table 5).

Finally, the peptides were transferred into water. Parameters characterizing the solvated systems are shown in Table 6. During 2.4-ns (tgvp) and 2.18-ns (YPGDV) solvated simulations without NOE constraints ("free dynamics") dihedral angles and intramolecular distances were monitored. Results are shown in Tables 1 and 2 (intranuclear distances) and Tables 3 and 4 (dihedral angles). Figures 1 and 2 (dashed lines) show the dihedral angle distribution functions for dynamics without constraints. The average distances of the hydrogen bonds are given in Table 5.

B. Dipolar Correlation Functions. The solvated simulations served primarily to calculate the dipolar correlation functions of a set of internuclear distances in both systems. Figures 3a–d and 4a–d show the total dipolar correlation functions of a subset of internuclear distance vectors in tgvp and YPGDV, respectively, together with the corresponding distance parts and angular parts.

(54) Press, W. H.; Flannery, B. P.; Teukolsky, S. A.; Vetterling, W. T. *Numerical Recipes. The Art of Scientific Computing*; Cambridge University Press: Cambridge, 1986.
(55) Zwanzig, R.; Ailawadi, N. *Phys. Rev.* **1969**, *182*, 280–283.
(56) Wüthrich, K. *NMR of Proteins and Nucleic Acids*; Wiley-Interscience: New York, 1986; Chapter 7.
(57) Sterk, H. Unpublished results.
(58) Bystrov, V. F.; Ivanov, V. T.; Portnova, S. L.; Balashova, T. A.; Ovchinnikov, Yu. A. *Tetrahedron* **1973**, *29*, 873–877.

Table 3. Results of Folding tgvp and Free Dynamics: Comparison of Simulated Average ϕ-Angles with NMR Data[a]

		NMR data[b]			
residue	angle	$^3J_{N\alpha}$/Hz	ϕ/deg	200-ps MD-tar ϕ/deg	2.4-ns free MD ϕ/deg
^{1}Cys	ϕ_1	8.6	−160, −80	−82.6 ± 8.4	−90.1 ± 26.0
^{2}Tyr	ϕ_2	8.9	−145, −95	−126.0 ± 11.4	−126.7 ± 24.5
^{3}Phe	ϕ_3	7.5	−155, −85, 70, 50	23.6 ± 24.6	22.3 ± 23.7
^{4}Gln	ϕ_4	6.2	−155, −85, 70, 50	61.1 ± 5.9	66.2 ± 11.7
^{5}Asn	ϕ_5	8.8	−145, −95, 70, 50	−78.3 ± 9.7	−89.1 ± 23.2
^{6}Cys	ϕ_6	6.4	−165, −75, 90, 30	−90.8 ± 11.7	−96.1 ± 21.6
^{8}Lys	ϕ_8	7.2	−165, −75, 80, 40	−52.3 ± 10.7	−37.6 ± 38.9

[a] The values in column 4 are derived from the ^3J coupling constants using the Karplus equation.[58] [b] From ref 57.

Table 4. Results of Folding YPGDV and Free Dynamics: Comparison of Literature and Average Simulation Data for ϕ- and ψ-Angles of Residues 2 and 3 of a Type II β-Turn

residue	angle	lit.[46]	lit.[27]	200-ps MD-tar	2.18-ns free MD
^{2}Pro	ϕ_2	−60°	−89°	−44.1° ± 6.1°	−54.5° ± 13.9°
^{2}Pro	ψ_2	120°	120°	90.4° ± 5.0°	127.2° ± 16.6°
^{3}Gly	ϕ_3	90°	90°	64.4° ± 8.6°	36.9° ± 112.2°
^{3}Gly	ψ_3	0°	0°	16.9° ± 12.3°	−72.0° ± 66.8

The motional parameters (correlation times and generalized order parameters) referred to in the following have been obtained by fitting the simulated correlation functions to the target functions described in the Programs and Methods section. Data are shown in Tables 7 and 8.

Distance Correlation Functions. The distance parts for both systems complete the major part of their decay on a subpicosecond time scale. The correlation times for this rapid initial decay are smaller than 100 fs; only for $d_{\alpha\alpha}^{GG}(\beta,\alpha)$ in tgvp a greater value (190 fs) is observed. (The numbering of residues in tgvp is the following: Gly$^\gamma$-Gly$^\beta$-Gly$^\alpha$-Cys^1-Tyr^2-Phe^3-Gln^4-Asn^5-Cys^6-Pro^7-Lys^8-Gly^9-NH_2.) In almost all cases a second time scale with correlation times between 1 and 18 ps follows. A further considerably slower decay (correlation times as long as 75 ps) occurs for several distance correlation functions, but the corresponding order parameter is always greater than 0.97; only for $d_{\alpha N}^{KG}(8,9)$ in tgvp (outside the ring) the order parameter for the slow correlation time (47 ps) is 0.93. The magnitude of the asymptotic value of the distance correlation function is correlated with the validity of the product approximation (see below).

Total and Orientational Correlation Functions. In the case of the angular and the total correlation functions the multiexponential character is more pronounced. The initial femtosecond time scale decay is followed by slower processes with non-negligible amplitudes. The corresponding order parameters of $C^{DD}(t)$ and $C_{rot}^{DD}(t)$ of both peptides are between 0.84 and 0.97; only for $d_{\alpha\alpha}^{GG}(\beta,\alpha)$, which lies outside the ring in tgvp, is it considerably lower (0.70). The intermediate correlation times are in the interval [0.7 ps, 13 ps], and even the slowest orientational correlation times τ_{snr} cover a rather broad range (tgvp, 130–292 ps; YPGDV, 62–141 ps). The slowest correlation times of the angular correlation function and of the total correlation function of a given NOE are quite similar, as can be seen in Tables 7 and 8.

Product Approximation. The validity of the product approximation (eq 7) has been investigated by comparing the product of the (independently averaged) angular and distance part to the total dipolar correlation function. Plots of a subset are shown in Figures 3e–h (tgvp) and 4e–h (YPGDV). For all the NOEs analyzed the average relative error (eq 22) is given in Tables 9 and 10. In order to illustrate the correlation between the product approximation error and the asymptotic value of the distance correlation function, $\Pi_i S_{dis,i}^2$ (cf. eq 23) is also listed. The average relative error does not exceed 0.9% (tgvp) or 1.5% (YPGDV), respectively, with the exception of $d_{\alpha N}^{KG}(8,9)$ (outside the ring in tgvp), which exhibits a 4.1% error (Figure 3h) and the lowest asymptotic value for a distance correlation function observed in tgvp. The smallest relative errors are observed for NOEs with very well correlated distances (e.g. Figure 3, parts b and f), and the error will vanish if the internuclear distance does not fluctuate at all. This is not surprising, because in this case $C_{dis}^{DD}(t)$ is equal to 1 for all times t.

A discussion of the separability issue in terms of radial and angular order parameters has recently been given by R. Brüschweiler et al.,[26] based on their molecular dynamics study of the decapeptide antamanide. They also find elongation and rotation separable to a good approximation.

Effects on the Calibration of Distances. Relying on these findings, in particular on the validity of the product approximation and the multiexponential characteristic of the correlation functions, we tried to generalize the r^{-6}-law in such a way that internal motions are accounted for.

The general form of the non-normalized distance correlation function used here is

$$C_{dis}^{DD}(t) = \overline{r^{-6}} \prod_n [S_{dis,n}^2 + (1 - S_{dis,n}^2)e^{-t/\tau_{dis,n}}] \qquad (32)$$

which is equal to

$$C_{dis}^{DD}(t) = \overline{r^{-6}} \prod_n S_{dis,n}^2 + \overline{r^{-6}} \sum_n a_n e^{-t/\tau'_{dis,n}} \qquad (33)$$

where the coefficients a_n stand for products of order parameters $S_{dis,i}^2$ or $(1 - S_{dis,i}^2)$, respectively, and $\tau'_{dis,n}$ is a combined correlation time formed according to

$$\tau'^{-1}_{dis,n} = \sum_i c_i \tau^{-1}_{dis,i} \qquad (34)$$

with c_i either 1 or 0. As shown in the appendix, the second term in eq 33 makes a very small contribution to the spectral density and will be neglected here. In other words, we retain only the asymptotic part of the distance correlation function, which we denote in the following simply with S_{dis}^2:

$$C_{dis,asymp}^{DD} = \overline{(r^{-3})^2} = \overline{r^{-6}} \prod_n S_{dis,n}^2 \equiv \overline{r^{-6}} S_{dis}^2 \qquad (35)$$

For the angular correlation function an analogous expression holds,

$$C_{rot}^{DD}(t) = \sum_m b_m e^{-t/\tau'_{rot,m}} \qquad (36)$$

where b_m again collects the angular order parameters and $\tau'_{rot,m}$ the rotational correlation times including τ_{snr}. For an appropriate example see eq 26. On the basis of this general form of the rotational correlation function, the rotational part of the total cross relaxation rate constant (eq 10) is given by the sum

$$F = \sum_m b_m f_m(\tau'_{rot,m}) \qquad (37)$$

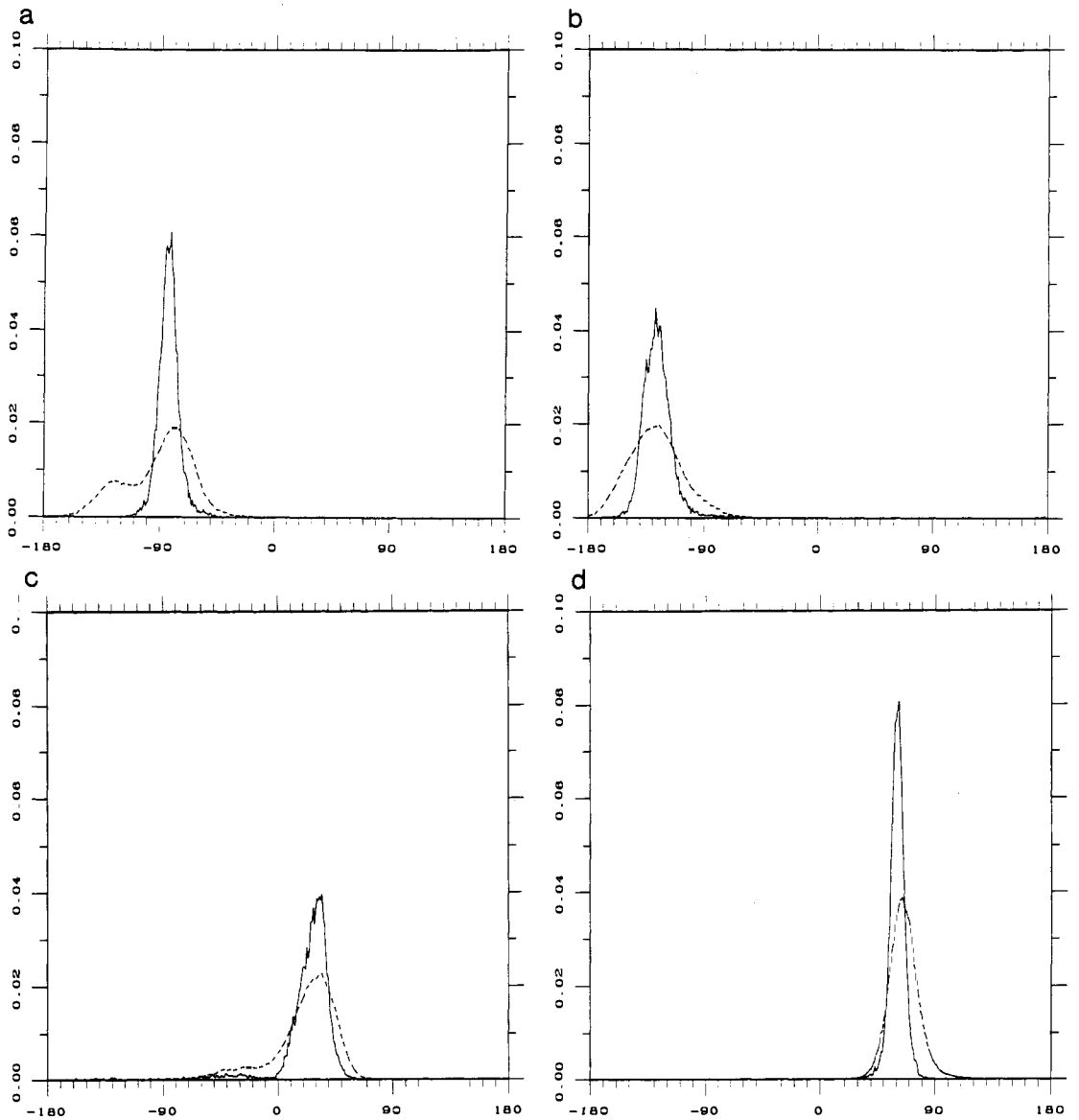

Figure 1. Distribution functions of main chain dihedral angles in tgvp: continuous lines (—) 200-ps MD-tar; dashed lines (- - -) 2.4-ns free MD; (a) ϕ_1; (b) ϕ_2; (c) ϕ_3; and (d) ϕ_4.

with the partial cross relaxation rate constants $f_m(\tau'_{\mathrm{rot},m})$ given by eq 11. As a consequence, the generalized form of eq 12 now reads

$$\frac{\sigma_{ij}}{\sigma_{kl}} = \frac{\overline{(r_{ij}^{-3})^2}}{\overline{(r_{kl}^{-3})^2}} \frac{F_{ij}}{F_{kl}} \tag{38}$$

If the extreme narrowing limit, i.e. $\tau \ll (1/\omega)$, holds for all τ'_{rot}, where ω is either $(\omega_I + \omega_S)$ or $(\omega_I - \omega_S)$, expression 11 simplifies to $5\tau_{\mathrm{rot}}$, which in its turn implies

$$F = 5\sum_m b_m \tau'_{\mathrm{rot},m} \tag{39}$$

Substituting expressions 35 and 39 into eq 38, we obtain

$$\frac{\sigma_{ij}}{\sigma_{kl}} = \frac{\overline{r_{ij}^{-6}}}{\overline{r_{kl}^{-6}}} \frac{(S^2_{\mathrm{dis}})_{ij}(\sum_m b_m \tau'_{\mathrm{rot},m})_{ij}}{(S^2_{\mathrm{dis}})_{kl}(\sum_m b_m \tau'_{\mathrm{rot},m})_{kl}} \tag{40}$$

As shown in the appendix, only the leading term in the respective sums,

$$S^2_{\mathrm{rot}}\tau_{\mathrm{snr}} \equiv (\prod_m S^2_{\mathrm{rot},m})\tau_{\mathrm{snr}} \tag{41}$$

is of practical importance. Thus, we obtain

$$\frac{\sigma_{ij}}{\sigma_{kl}} = \frac{\overline{r_{ij}^{-6}}}{\overline{r_{kl}^{-6}}} \frac{S^2_{ij}}{S^2_{kl}} \frac{\tau_{\mathrm{snr},ij}}{\tau_{\mathrm{snr},kl}} \tag{42}$$

where $S^2 = S^2_{\mathrm{dis}}S^2_{\mathrm{rot}}$ within the framework of the product approximation. This equation differs from the commonly used expression, eq 13, for deriving internuclear distances by two modifying cofactors: the ratio of the total order parameters S^2_{ij}/S^2_{kl} and the ratio of the slowest angular correlation times $\tau_{\mathrm{snr},ij}/\tau_{\mathrm{snr},kl}$. As we have shown in Tables 7 and 8, S^2 and τ_{snr} are not universal, but rather specific for the underlying NOE. Thus, the two ratios are far from unity. Performing a "worst case" analysis, we find $\max(S^2_{ij}/S^2_{kl}) = 1.42$, $\max(\tau_{\mathrm{snr},ij}/\tau_{\mathrm{snr},kl}) = 2.25$ for tgvp and $\max(S^2_{ij}/S^2_{kl}) = 1.23$, $\max(\tau_{\mathrm{snr},ij}/\tau_{\mathrm{snr},kl}) = 2.28$ for YPGDV.

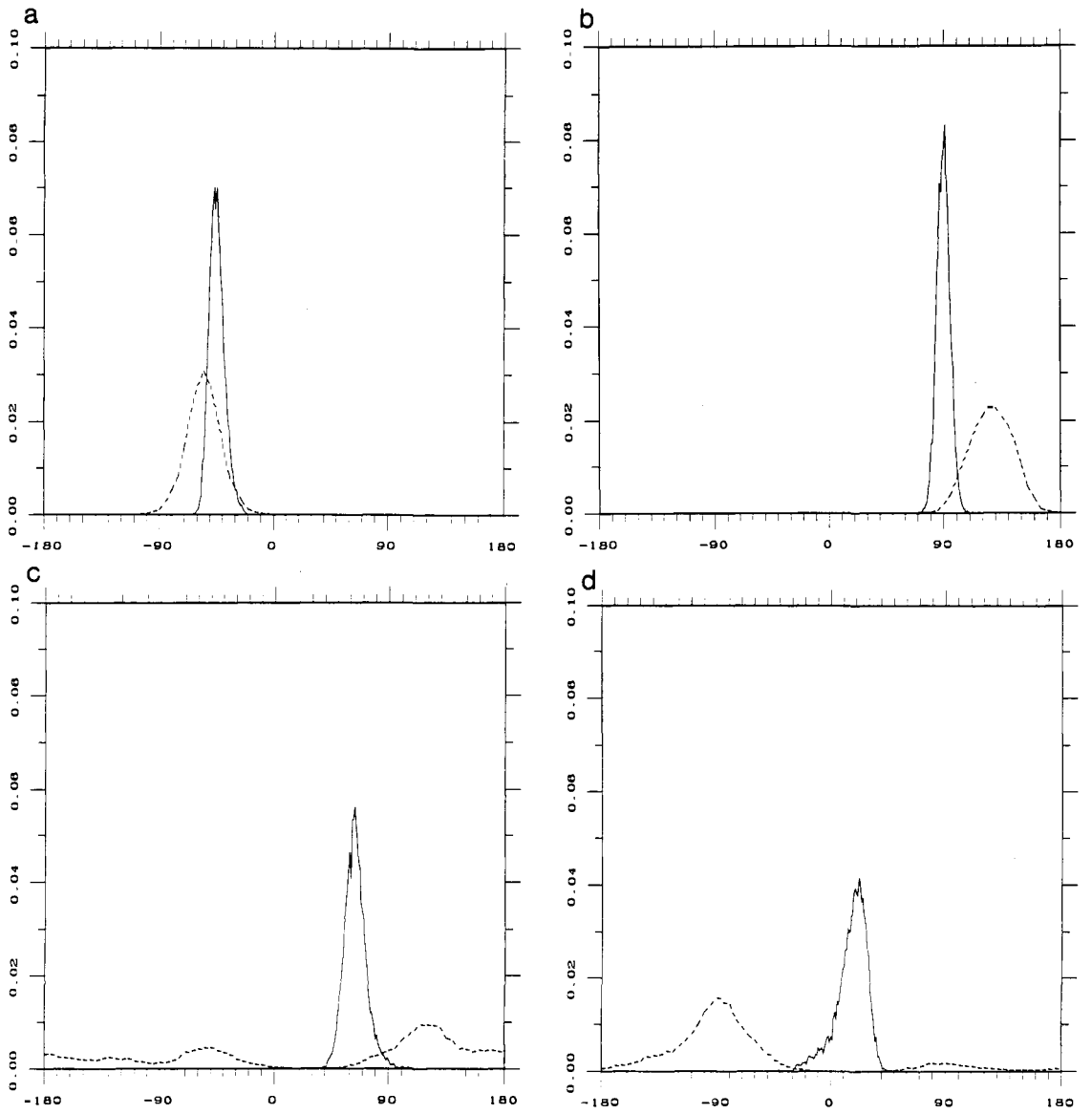

Figure 2. Distribution functions of main chain dihedral angles in YPGDV: continuous lines (—) 200-ps MD-tar; dashed lines (- - -) 2.18-ns free MD; (a) ϕ_2; (b) ψ_2; (c) ϕ_3; and (d) ψ_3.

Table 5. Average O–H Distance of the Hydrogen Bonds in tgvp and YPGDV (in nm)

hydrogen bond	200-ps MD-tar	solvated simulation
tgvp: ^{3}PheCO–^{5}AsnNH	0.204 ± 0.014	0.208 ± 0.028
YPGDV: ^{1}TyrCO–^{4}AsnNH	0.196 ± 0.010	0.547 ± 0.137

Table 6. Parameters of the Solvated Systems

	tgvp	YPGDV
peptide atoms[a]	108	46
counterions	2	3
H_2O molecules	983	712
box size/nm^3	3.0 × 3.0 × 3.5	2.8 × 2.8 × 2.8

[a] No explicit hydrogen atoms on carbon atoms.

For the actual derivation of internuclear distances, however, the inverse sixth power of the respective ratio is taken. These are

$$(S_{ij}^2/S_{kl}^2)^{1/6}_{\text{worst case}} = 1.42^{1/6} = 1.06$$

$$(\tau_{\text{snr},ij}/\tau_{\text{snr},kj})^{1/6}_{\text{worst case}} = 2.25^{1/6} = 1.14$$

for tgvp and

$$(S_{ij}^2/S_{kl}^2)^{1/6}_{\text{worst case}} = 1.23^{1/6} = 1.04$$

$$(\tau_{\text{snr},ij}/\tau_{\text{snr},kl})^{1/6}_{\text{worst case}} = 2.28^{1/6} = 1.15$$

for YPGDV.

Discussion

The structures of *N*-triglycin[Lys^8]vasopressin and YPGDV have been modeled with the restrained molecular dynamics method. A small number of NOE constraints have been used with small force constants in the range of 0.5% (1% or 2.5% in a few cases) of a covalent bond of the GROMOS force field. This becomes feasible by the application of time-averaged distance constraints. As the constraints have to be satisfied on average only, the systems retain their genuine dynamical behavior to a greater extent as compared to the use of conventional distance constraints.[59,60] Nevertheless, the modeled structures are compatible with other independently determined experimental data.

(59) Schmitz, U.; Kumar, A.; James, T. L. *J. Am. Chem. Soc.* **1992**, *114*, 10654–10656.
(60) Pearlman, D. A.; Kollman, P. A. *J. Mol. Biol.* **1991**, *220*, 429–457.

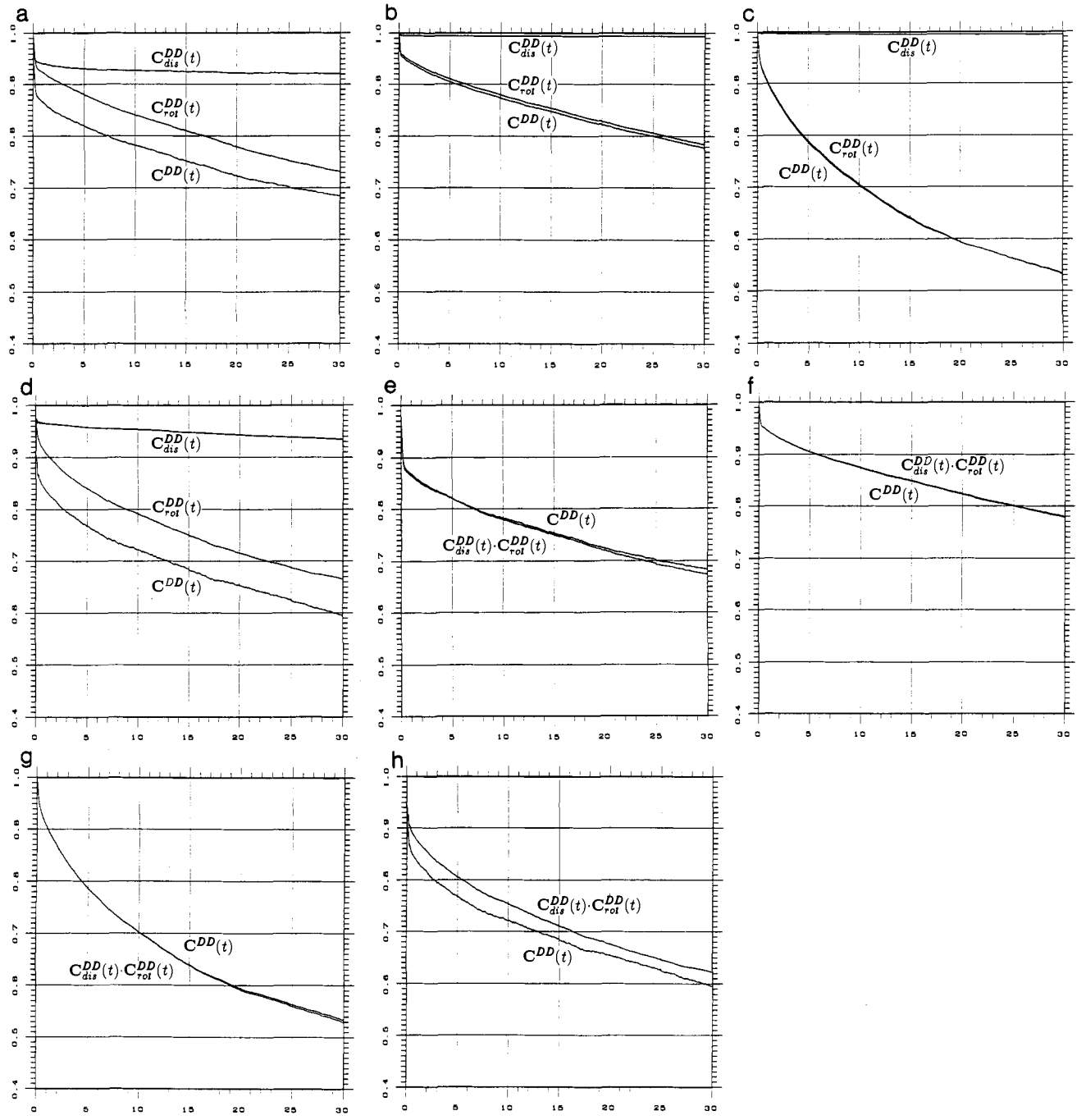

Figure 3. Normalized dipolar correlation functions of $d^{CC}_{\alpha\alpha}(1,6)$, $d^{CP}_{\alpha\delta}(6,7)$, $d^{GG}_{\alpha\alpha}(\beta,\alpha)$, and $d^{KG}_{\alpha N}(8,9)$ (tgvp) plotted against time in picoseconds (trajectory length 2.40 ns, time window 30 ps, sampling interval 0.02 ps): (a–d) total dipolar correlation functions (lower curves in all diagrams), corresponding angular parts (middle curves), and distance parts (upper curves); in b and c the total dipolar correlation function and the angular part nearly coincide; (e–h) total dipolar correlation functions and products of angular and distance parts.

During the solvated simulations the two peptides exhibit entirely different dynamical behavior. The ring moiety of tgvp is very rigid, whereas YPGDV loses the type II β-turn-specific conformation. A profound study of the behavior of YPGDV during a 2.2-ns solvated simulation has been reported by D. J. Tobias et al.[61] It is evident that the dynamic behavior of YPGDV contrasts with the dynamic behavior of a type II β-turn in a native protein. For the present investigation it served primarily as a model system with high mobility.

As this analysis deals with small systems, it is restricted to NOEs with short sequence distances. There is only one long-range NOE ($d^{CC}_{\alpha\alpha}(1,6)$ in tgvp). However, the motion of this distance vector is restricted by the adjacent disulfide bond and therefore not truly characteristic for long-range NOEs.

The striking differences between the two systems with regard to their dynamical behavior do not reflect themselves in the correlation functions. With respect to the general shape of the correlation functions the differences within a system exceed those between them.

The foundations of the commonly used r^{-6}-law for distance determination from NOE data have been investigated. The analysis focused on the basic assumptions involved in the derivation of the r^{-6}-law: (1) Can elongation and rotation of an internuclear distance vector be considered as independent processes? (2) Does elongation occur on a time scale faster than rotation? (3) Is the reorientational motion of all internuclear distance vectors describable by a uniform model, i.e. a model with parameters specific

(61) Tobias, D. J.; Mertz, J. E.; Brooks, C. L., III. *Biochemistry* **1991**, *30* (24), 6054–6058.

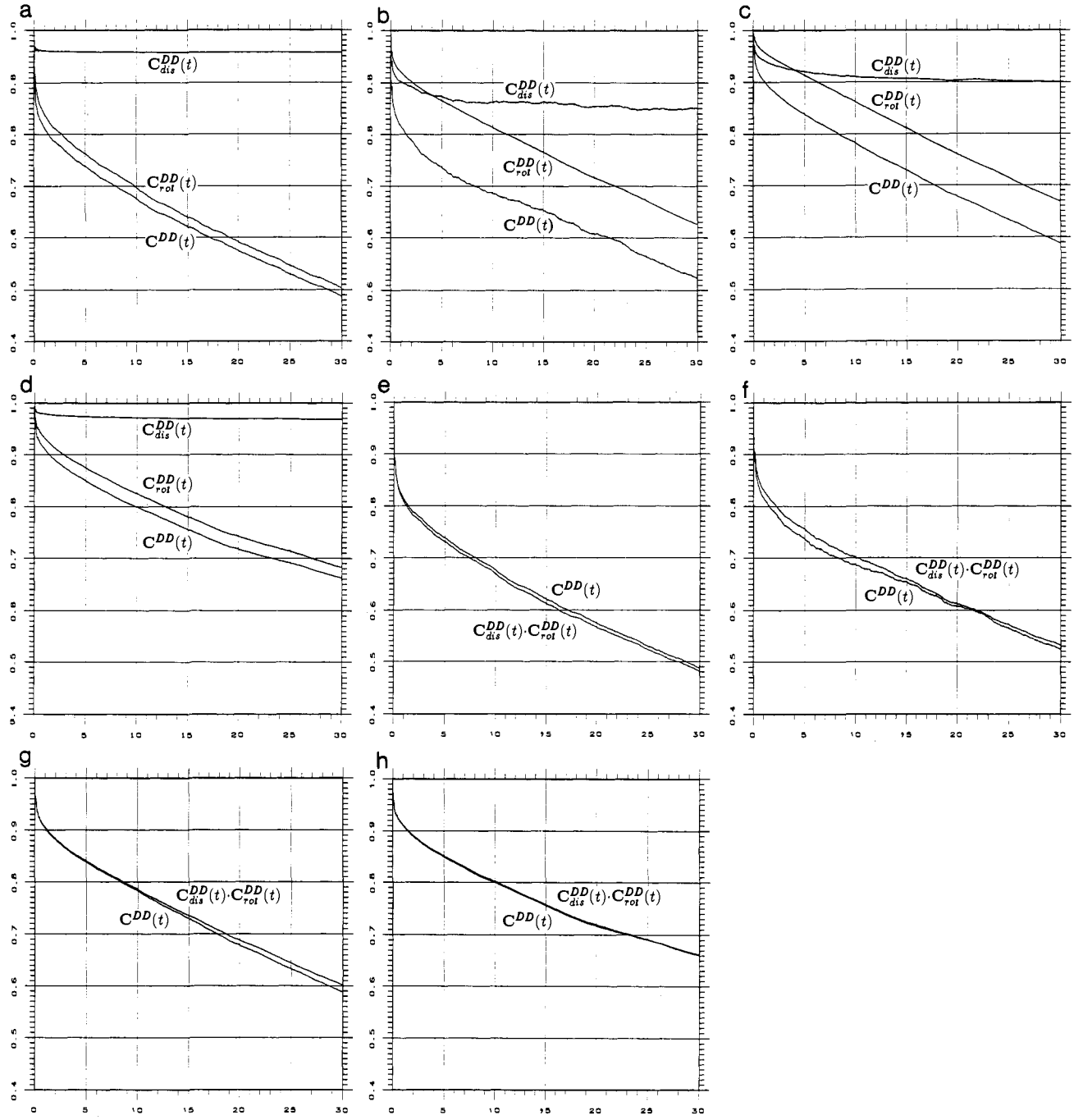

Figure 4. Normalized dipolar correlation functions of $d^{PG}_{\alpha N}(2,3)$, $d^{GD}_{NN}(3,4)$, $d^{PD}_{\alpha N}(2,4)$, and $d^{DV}_{NN}(4,5)$ (YPGDV) plotted against time in picoseconds (trajectory length 2.18 ns, time window 30 ps, sampling interval 0.02 ps): (a–d) total dipolar correlation functions (lower curves in all diagrams), corresponding angular parts (middle curves), and distance parts (upper curves); (e–h) total dipolar correlation functions and products of angular and distance parts.

for the system as a whole and not specific for each single NOE? We summarize our findings in the following paragraphs.

(1) As mentioned in the theory section, a reasonable approach for simplifying the dipolar correlation function is a splitting in an overall and an internal part. This would apply to large systems, for which the influence of internal motions on the overall reorientation is usually negligible. For smaller systems a more intricate coupling between these two hierarchies of motion has to be expected. Under these circumstances no longer can a well-defined overall correlation time be expected, because local motions will act upon the overall tumbling behavior. In fact the τ_{snr} correlation times show a significant diversity which cannot be interpreted in terms of insufficient averaging. It could of course be attributed to the anisotropy of tumbling. As mentioned in the Programs and Methods section, it was our intention to use as few parameters as possible in our target functions. Therefore, we characterized the spatially not restricted component (snr) of molecular motion with a single parameter, τ_{snr}. This requires τ_{snr} to be specific for a given NOE.

In contrast to the factoring in an overall and an internal part, the derivation of the r^{-6}-law uses a different product approximation, namely, a splitting into a distance and an angular part, which reflects the physical reality to an even smaller extent. Surprisingly, this kind of factoring method does not yield relative errors greater than 4.1% for the two peptide systems studied. The size of the error is coupled with the asymptotic value of the distance correlation function. Taking the asymptotic value of the distance correlation function as a measure for distance fluctuations, it

Table 7. Correlation Times and Generalized Order Parameters of Total, Angular, and Distance Correlation Functions for Nine Internuclear Distance Vectors in tgvp[a]

NOE	correlation function	target function	motional parameters		$\sum_{t=0}^{T}[g(t)-C(t)]^2$
			correlation times (ps)	corresponding order parameters	
$d_{\alpha\alpha}^{CC}(1,6)$	$C^{DD}(t)$	eq 25	0.124, 6.14, 159	0.877, 0.937, 0.0	4.143×10^{-3}
	$C_{rot}^{DD}(t)$	eq 25	0.145, 5.83, 150	0.935, 0.953, 0.0	1.878×10^{-3}
	$C_{dis}^{DD}(t)$	eq 23, $i = 3$	0.091, 2.20, 29.2	0.947, 0.985, 0.981	0.401×10^{-3}
$d_{\alpha N}^{CY}(1,2)$	$C^{DD}(t)$	eq 25	0.073, 3.23, 195	0.872, 0.956, 0.0	5.097×10^{-3}
	$C_{rot}^{DD}(t)$	eq 25	0.113, 3.79, 196	0.894, 0.957, 0.0	3.940×10^{-3}
	$C_{dis}^{DD}(t)$	eq 23, $i = 2$	0.015, 5.50	0.968, 0.997	0.235×10^{-3}
$d_{\alpha N}^{YF}(2,3)$	$C^{DD}(t)$	eq 25	0.071, 2.37, 226	0.876, 0.938, 0.0	4.136×10^{-3}
	$C_{rot}^{DD}(t)$	eq 25	0.108, 2.72, 234	0.901, 0.941, 0.0	2.646×10^{-3}
	$C_{dis}^{DD}(t)$	eq 23, $i = 2$	0.021, 6.86	0.965, 0.995	0.396×10^{-3}
$d_{\alpha N}^{FQ}(3,4)$	$C^{DD}(t)$	eq 25	0.060, 7.33, 128	0.875, 0.941, 0.0	9.482×10^{-3}
	$C_{rot}^{DD}(t)$	eq 25	0.109, 12.18, 141	0.900, 0.915, 0.0	8.779×10^{-3}
	$C_{dis}^{DD}(t)$	eq 23, $i = 2$	0.016, 12.11	0.966, 0.995	0.247×10^{-3}
$d_{\alpha N}^{QN}(4,5)$	$C^{DD}(t)$	eq 25	0.104, 4.77, 133	0.946, 0.960, 0.0	1.165×10^{-3}
	$C_{rot}^{DD}(t)$	eq 25	0.113, 4.069, 130	0.956, 0.966, 0.0	0.902×10^{-3}
	$C_{dis}^{DD}(t)$	eq 23, $i = 2$	0.021, 4.365	0.992, 0.997	0.052×10^{-3}
$d_{\alpha N}^{NC}(5,6)$	$C^{DD}(t)$	eq 25	0.092, 6.99, 237	0.875, 0.930, 0.0	6.608×10^{-3}
	$C_{rot}^{DD}(t)$	eq 25	0.148, 9.53, 292	0.899, 0.908, 0.0	4.847×10^{-3}
	$C_{dis}^{DD}(t)$	eq 23, $i = 2$	0.017, 6.20	0.967, 0.997	0.204×10^{-3}
$d_{\alpha\delta}^{CP}(6,7)$	$C^{DD}(t)$	eq 25	0.114, 3.91, 177	0.956, 0.964, 0.0	0.599×10^{-3}
	$C_{rot}^{DD}(t)$	eq 25	0.124, 3.94, 178	0.960, 0.967, 0.0	0.576×10^{-3}
	$C_{dis}^{DD}(t)$	eq 23, $i = 2$	0.037, 4.60	0.996, 0.998	0.009×10^{-3}
$d_{\alpha\alpha}^{GG}(\beta,\alpha)$	$C^{DD}(t)$	eq 25	0.370, 10.14, 141	0.925, 0.701, 0.0	5.068×10^{-3}
	$C_{rot}^{DD}(t)$	eq 25	0.381, 10.19, 133	0.928, 0.706, 0.0	4.865×10^{-3}
	$C_{dis}^{DD}(t)$	eq 23, $i = 2$	0.190, 18.10	0.997, 0.997	0.016×10^{-3}
$d_{\alpha N}^{KG}(8,9)$	$C^{DD}(t)$	eq 25	0.067, 3.29, 109	0.867, 0.906, 0.0	4.812×10^{-3}
	$C_{rot}^{DD}(t)$	eq 25	0.144, 6.37, 132	0.927, 0.897, 0.0	4.488×10^{-3}
	$C_{dis}^{DD}(t)$	eq 23, $i = 2$	0.0006, 46.96	0.966, 0.932	0.949×10^{-3}

[a] The target functions are introduced in the Programs and Methods section. The sums of least squares (cf. Programs and Methods section are given in the last column.

seems plausible that higher asymptotic values, i.e. smaller fluctuations, are in accordance with a better validity of the product approximation. Of course, these findings have to be ascertained by further studies on other systems.

(2) Elongation does not occur on time scales faster than rotation. Nevertheless, it will be possible to write an expression for the total spectral density containing *no* distance correlation times with acceptable approximation. This is due to two reasons: (1) The fastest processes give rise to very small contributions to the spectral density because their time constants are extremely small (femtosecond range). (2) The slower processes are generally associated with generalized order parameters S_i^2 close to 1.0. Thus, their contribution is scaled by $(1 - S_i^2)$, making it negligible, too. The error resulting from dropping the time-dependent part of the distance correlation function is at most 1.9% (tgvp) or 1.6% (YPGDV), respectively.

(3) The rotational correlation functions of different internuclear vectors show a significant diversity. In other words, site-specific internal motions contribute to the angular part of the total dipolar correlation function. Distances obtained by the commonly used r^{-6}-law will be subject to systematic errors as large as 15%, which is 1 order of magnitude greater than the product approximation error. Thus, individual correlation times appear to be the major source of error in NOE-derived distances, as far as the influence of molecular motion is concerned.

Relying on the product approximation, a modified calibration formula is suggested. It introduces a scaling factor that compensates for the error resulting from individual correlation times and individual amplitudes of internal motions. This formula (eq 42) contains the slowest rotational correlation times of the NOE of interest and the calibration standard, weighted with the generalized order parameters of the corresponding dipolar correlation functions.

Concluding, we point out that the findings of this study cannot be simply transferred to proteins, which exhibit a greater variety of motional processes. Provided that the factoring holds for proteins as well, one may conjecture an empirical correspondence between the magnitude of the rotational correlation times and generalized order parameters on the one hand and the type of structural elements involved in the NOE coupling on the other hand. This would pave the way for a class-specific calibration of NOEs. Investigations along these lines are currently in progress.

Acknowledgment. Helpful and valuable suggestions from the referee are gratefully acknowledged. This work was supported by the Austrian Fonds zur Förderung der wissenschaftlichen Forschung under project no. P7932.

Appendix

The expressions for the distance correlation function $C_{dis}^{DD}(t)$ and the orientational correlation function $C_{rot}^{DD}(t)$ used here give rise to a rather complicated expression for the spectral density. As a simple calibration formula is desirable, approximations are introduced in the derivation of eq 42. Here we show the background for these approximations in a general form and give a quantitative analysis.

The normalized distance correlation function and the orientational correlation function are given by

$$C_{dis}^{DD}(t) = \prod_i [S_{dis,i}^2 + (1 - S_{dis,i}^2)e^{-t/\tau_{dis,i}}] \qquad (43)$$

Table 8. Correlation Times and Generalized Order Parameters of Total, Angular, and Distance Correlation Functions for Seven Internuclear Distance Vectors in YPGDV[a]

NOE	correlation function	target function	motional parameters: correlation times (ps)	motional parameters: corresponding order parameters	$\sum_{t=0}^{T}[g(t)-C(t)]^2$
$d_{\alpha N}^{PG}(2,3)$	$C^{DD}(t)$	eq 25	0.068, 1.72, 61.7	0.857, 0.926, 0.0	5.930×10^{-3}
	$C_{rot}^{DD}(t)$	eq 25	0.117, 2.19, 61.8	0.877, 0.933, 0.0	5.812×10^{-3}
	$C_{dis}^{DD}(t)$	eq 23, $i = 2$	0.023, 4.15	0.962, 0.995	0.262×10^{-3}
$d_{NN}^{GD}(3,4)$	$C^{DD}(t)$	eq 25	0.055, 1.36, 77.0	0.876, 0.896, 0.0	32.56×10^{-3}
	$C_{rot}^{DD}(t)$	eq 25	0.053, 0.682, 78.6	0.960, 0.962, 0.0	5.624×10^{-3}
	$C_{dis}^{DD}(t)$	eq 23, $i = 2$	0.118, 4.99	0.910, 0.937	19.19×10^{-3}
$d_{\alpha\delta}^{YP}(1,2)$	$C^{DD}(t)$	eq 25	0.112, 4.67, 54.8	0.890, 0.906, 0.0	5.532×10^{-3}
	$C_{rot}^{DD}(t)$	eq 25	0.159, 9.85, 66.5	0.912, 0.854, 0.0	3.537×10^{-3}
	$C_{dis}^{DD}(t)$	eq 23, $i = 3$	0.044, 2.07, 74.5	0.976, 0.991, 0.970	0.189×10^{-3}
$d_{\alpha N}^{GD}(3,4)$	$C^{DD}(t)$	eq 25	0.095, 2.55, 67.5	0.897, 0.902, 0.0	5.970×10^{-3}
	$C_{rot}^{DD}(t)$	eq 25	0.115, 2.09, 63.8	0.918, 0.924, 0.0	5.249×10^{-3}
	$C_{dis}^{DD}(t)$	eq 23, $i = 2$	0.028, 7.828	0.978, 0.986	1.133×10^{-3}
$d_{\alpha N}^{PD}(2,4)$	$C^{DD}(t)$	eq 25	0.097, 1.05, 70.8	0.942, 0.955, 0.0	1.255×10^{-3}
	$C_{rot}^{DD}(t)$	eq 24	0.194, 81.0	0.973, 0.0	6.238×10^{-3}
	$C_{dis}^{DD}(t)$	eq 23, $i = 3$	0.105, 2.27, 11.4	0.957, 0.968, 0.971	0.869×10^{-3}
$d_{NN}^{DV}(4,5)$	$C^{DD}(t)$	eq 25	0.161, 11.0, 142	0.922, 0.880, 0.0	7.803×10^{-3}
	$C_{rot}^{DD}(t)$	eq 25	0.211, 12.9, 141	0.942, 0.887, 0.0	4.684×10^{-3}
	$C_{dis}^{DD}(t)$	eq 23, $i = 3$	0.044, 1.39, 15.4	0.983, 0.992, 0.991	0.148×10^{-3}
$d_{\alpha N}^{DV}(4,5)$	$C^{DD}(t)$	eq 25	0.089, 6.46, 102	0.839, 0.876, 0.0	9.955×10^{-3}
	$C_{rot}^{DD}(t)$	eq 25	0.130, 7.02, 105	0.865, 0.865, 0.0	8.392×10^{-3}
	$C_{dis}^{DD}(t)$	eq 23, $i = 3$	0.016, 0.888, 75.2	0.963, 0.997, 0.988	0.273×10^{-3}

[a] The target functions are introduced in the Programs and Methods section. The sums of least squares (cf. Programs and Methods section) are given in the last column.

Table 9. Average Relative Error Due to the Product Approximation of the Dipolar Correlation Function and Asymptotic Values of the Distance Part of the Dipolar Correlation Function (tgvp)

NOE	⟨error(PA)⟩	$\prod_i S_{dis,i}^2$
$d_{\alpha\alpha}^{CC}(1,6)$	–0.47%	0.914
$d_{\alpha N}^{CY}(1,2)$	–0.77%	0.965
$d_{\alpha N}^{YF}(2,3)$	–0.53%	0.960
$d_{\alpha N}^{FQ}(3,4)$	–0.89%	0.961
$d_{\alpha N}^{QN}(4,5)$	0.11%	0.989
$d_{\alpha N}^{NC}(5,6)$	–0.75%	0.964
$d_{\alpha\delta}^{CP}(6,7)$	0.11%	0.994
$d_{\alpha\alpha}^{GG}(\beta,\alpha)$	–0.25%	0.994
$d_{\alpha N}^{KG}(8,9)$	4.10%	0.901

Table 10. Average Relative Error Due to the Product Approximation of the Dipolar Correlation Function and Asymptotic Values of the Distance Part of the Dipolar Correlation Function (YPGDV)

NOE	⟨error(PA)⟩	$\prod_i S_{dis,i}^2$
$d_{\alpha N}^{PG}(2,3)$	–1.17%	0.957
$d_{NN}^{GD}(3,4)$	1.53%	0.853
$d_{\alpha\delta}^{YP}(1,2)$	1.00%	0.938
$d_{\alpha N}^{GD}(3,4)$	–0.04%	0.965
$d_{\alpha N}^{PD}(2,4)$	0.97%	0.899
$d_{NN}^{DV}(4,5)$	0.16%	0.967
$d_{\alpha N}^{DV}(4,5)$	–1.39%	0.948

and

$$C_{rot}^{DD}(t) = \prod_j [S_{rot,j}^2 + (1 - S_{rot,j}^2)e^{-t/\tau_{rot,j}}]e^{-t/\tau_{snr}} \quad (44)$$

Evaluating the products and splitting off a *leading term* in both cases, we can rewrite these equations:

$$C_{dis}^{DD}(t) = \prod_i S_{dis,i}^2 + \sum_k a_k e^{-t/\tau'_{dis,k}} \quad (45)$$

$$C_{rot}^{DD}(t) = \prod_j S_{rot,j}^2 e^{-t/\tau_{snr}} + \sum_l b_l e^{-t/\tau'_{rot,l}} \quad (46)$$

Applying the product approximation eq 7, we obtain

$$C^{DD}(t) = \prod_i S_{dis,i}^2 \prod_j S_{rot,j}^2 e^{-t/\tau_{snr}} + \prod_i S_{dis,i}^2 \sum_l b_l e^{-t/\tau'_{rot,l}} + \prod_j S_{rot,j}^2 \sum_k a_k e^{-t(\tau'^{-1}_{dis,k} + \tau^{-1}_{snr})} + \sum_k \sum_l a_k b_l e^{-t(\tau'^{-1}_{dis,k} + \tau'^{-1}_{rot,l})} \quad (47)$$

The two peptides studied here fulfill the extreme narrowing limit quite well; that is, the condition $\tau \ll (1/\omega)$ is valid for all

Table 11. Relative Contribution of the Terms I, II, III, and IV (Eq 48) to the Total Spectral Density (tgvp)

NOE	I	II	III	IV
$d_{\alpha\alpha}^{CC}(1,6)$	99.49	0.1906	0.3184	0.0038
$d_{\alpha N}^{CY}(1,2)$	99.90	0.092 27	0.008 458	0.000 21
$d_{\alpha N}^{YF}(2,3)$	99.91	0.077 02	0.014 57	0.000 34
$d_{\alpha N}^{FQ}(3,4)$	99.22	0.7422	0.039 83	0.0020
$d_{\alpha N}^{QN}(4,5)$	99.88	0.1104	0.009 894	0.000 19
$d_{\alpha N}^{NC}(5,6)$	99.67	0.3254	0.006 434	0.000 45
$d_{\alpha\delta}^{CP}(6,7)$	99.92	0.076 84	0.005 128	0.000 092
$d_{\alpha\alpha}^{GG}(\beta,\alpha)$	97.05	2.906	0.035 40	0.0060
$d_{\alpha N}^{KG}(8,9)$	97.57	0.5251	1.868	0.034

correlation times. Thus, the Fourier transform reduces to a simple integral over the correlation function:

$$\int_0^\infty C^{DD}(t) = \underbrace{\prod_i S^2_{dis,i} \prod_j S^2_{rot,j} \tau_{snr}}_{I} + \underbrace{\prod_i S^2_{dis,i} \sum_l b_l \tau_{rot,l}}_{II} + \underbrace{\prod_j S^2_{rot,j} \sum_k a_k (\tau_{dis,k}^{-1} + \tau_{snr}^{-1})^{-1}}_{III} + \underbrace{\sum_k \sum_l a_k b_l (\tau_{dis,k}^{-1} + \tau_{rot,l}^{-1})^{-1}}_{IV} \quad (48)$$

The four terms in this expression have the following meaning: The first term stems from the leading terms of $C^{DD}_{dis}(t)$ and $C^{DD}_{rot}(t)$ and is expected to make up the major part of the spectral density (for data see Tables 11 and 12). The second and third term represent "first-order" correction terms, and the fourth term is a "second-order" correction term. Dropping the time-dependent part of the distance correlation function now means to keep only the terms I and II. The refined calibration formula eq 42 relies only on term I. We calculated the relative contribution of these terms to the total spectral density for all NOEs considered in this study. They are given in Tables 11 and 12.

Table 12. Relative Contribution of the terms I, II, III, and IV (Eq 48) to the Total Spectral Density (YPGDV)

NOE	I	II	III	IV
$d^{PG}_{\alpha N}(2,3)$	99.69	0.2730	0.033 58	0.0013
$d^{GD}_{NN}(3,4)$	99.54	0.036 71	0.4169	0.0029
$d^{YP}_{\alpha\delta}(1,2)$	96.24	2.153	1.546	0.062
$d^{GD}_{\alpha N}(3,4)$	99.56	0.2754	0.1566	0.0033
$d^{PD}_{\alpha N}(2,4)$	99.53	0.006 539	0.4624	0.000 40
$d^{DV}_{NN}(4,5)$	98.83	1.075	0.090 69	0.0062
$d^{DV}_{\alpha N}(4,5)$	98.50	0.9848	0.5040	0.011

It can be seen that for the two peptides, with regard to the spectral density, the total dipolar correlation function is well approximated by the product of the leading terms of the angular and the distance correlation function.